IAES International Journal of Robotics and Automation (IJRA)
Vol. 15, No. 2, June 2026, pp. 445~457
ISSN: 2722-2586, DOI: 10.11591/ijra.v15i2.pp445-457

Cascaded generalized predictive control for induction drives under constraints using particle swarm optimization

Rachid Amrouche[1], Noureddine Boumalha[2], Farid Ykhlef[1], Djilali Kouchih[1]
[1]Electronics Department, University of Blida 1, Blida, Algeria
[2]Automation Control Department, National Polytechnic School, Alger, Algeria

Article Info

Article history:

Received Oct 31, 2025
Revised Feb 21, 2026
Accepted Apr 1, 2026

Keywords:

Cascaded generalized predictive control
Constrained control
Induction motor drives
Particle swarm optimization
RST control

ABSTRACT

This paper presents a cascaded generalized predictive control (CGPC) strategy for induction motor drives under operational constraints, optimized through particle swarm optimization (PSO). In the proposed scheme, the outer loop regulates the motor speed, while the inner loop controls torque and flux, ensuring accurate multi-level regulation. PSO is employed to optimally tune the prediction horizon and weighting factors, enhancing robustness, transient response, and disturbance rejection. Unlike conventional GPC–PSO approaches that neglect explicit constraint handling, and linear matrix inequalities (LMI)-based model predictive controller (MPC) methods that impose high computational costs, the proposed CGPC–PSO achieves both constraint management and real-time efficiency. Moreover, compared with Neural-MPC strategies that require retraining for each system, the proposed method provides generalizable and adaptive control without sacrificing computational performance. Simulation results validate the effectiveness of the approach, demonstrating superior trajectory tracking, robustness against parameter variations, and improved dynamic performance compared with RST, LMI, and neural-MPC controllers. These findings position CGPC–PSO as a promising candidate for advanced induction motor drive applications.

Corresponding Author:

Rachid Amrouche
Electronics Department, University of Blida 1
Blida, Algeria
Email: rachamrouche1976@gmail.com

1. INTRODUCTION

Induction motor drives are extensively employed in modern industry owing to their robustness, efficiency, and cost-effectiveness. However, achieving high-performance control under nonlinear dynamics, parameter variations, and operational constraints remains a major challenge. Model-based predictive control (MPC) has emerged as a key technique in advanced control systems, primarily due to its strong setpoint tracking performance and inherent capacity to manage system constraints. Within the broad family of MPC approaches, generalized predictive control (GPC), first introduced by Clarke *et al.* [1], [2], remains one of the most robust and flexible methods. By minimizing a quadratic cost function, GPC enables effective control of systems characterized by time delays, non-minimum phase behavior, or complex dynamics [3], [4].

Several MPC-based approaches have been explored for induction motor drives. GPC optimized by particle swarm optimization (PSO) has been reported as an effective method for tuning predictive controller parameters. For example, Oliveira *et al.* [5] optimized GPC parameters using PSO but did not explicitly address input/output constraints, while He *et al.* [6] faced difficulties with real-time computation and robustness in perturbed multi-input multi-output (MIMO) environments. Similarly, linear matrix inequalities

(LMI)-based MPC methods, such as those proposed by Kim *et al.* [7], guarantee constraint satisfaction but impose high computational complexity, making real-time implementation impractical. Hybrid convex–LMI MPC approaches [8] attempt to reduce this burden, but they often deteriorate in highly nonlinear or cascaded structures.

Neural predictive control strategies also provide alternatives. Stiti *et al.* [9] proposed a neural predictive scheme requiring retraining for each system. Wang *et al.* [10] introduced neural–MPC variants that, despite their learning ability, lacked effective real-time adaptability under dynamic operating conditions.

The proposed cascaded generalized predictive control (CGPC) method optimized by PSO advances beyond these prior strategies in several key aspects. Unlike earlier PSO–GPC approaches, the CGPC–PSO explicitly manages input/output constraints while adapting online. Compared with LMI-based and hybrid convex–LMI MPC methods, it achieves both computational efficiency and robustness, ensuring real-time applicability. Furthermore, unlike neural predictive strategies that depend on retraining and exhibit limited adaptability, the CGPC–PSO provides a generalizable, flexible, and adaptive solution. Overall, the proposed method demonstrates clear advantages in computational performance, robustness, and adaptability, positioning it as a strong candidate for advanced induction motor drive applications.

The remainder of this paper is organized as follows: Section 2 presents the modeling of the induction motor and the fundamentals of GPC. Section 3 describes the proposed CGPC–PSO design methodology. Section 4 reports the simulation results and provides a comparative analysis with conventional approaches. Finally, Section 5 concludes the paper and outlines future research perspectives.

The proposed CGPC-PSO control framework can be extended to robotic applications such as actuator drives, autonomous vehicle propulsion systems, and multi-motor cooperative robots. Its adaptive optimization capability enables coordinated torque control and efficient power management, which are essential in advanced robotic systems.

2. METHOD

2.1. Dynamic modeling of the induction motor

The state-space (1) represents the dynamics of the induction motor [11].

$$\begin{cases} \frac{di_{\alpha s}}{dt} = -\frac{1}{\sigma L_s}\left(R_s + R_r\frac{L_m^2}{L_r^2}\right)i_{\alpha s} + \frac{1}{\sigma L_s}R_r\frac{L_m}{L_r^2}\Phi_{\alpha r} + \frac{1}{\sigma L_s}\omega\frac{L_m}{L_r^2}\Phi_{\beta r} + \frac{1}{\sigma L_s}V_{\alpha s} \\ \frac{di_{\beta s}}{dt} = -\frac{1}{\sigma L_s}\left(R_s + R_r\frac{L_m^2}{L_r^2}\right)i_{\beta s} - \frac{1}{\sigma L_s}\omega\frac{L_m}{L_r}\Phi_{\alpha r} + \frac{1}{\sigma L_s}R_r\frac{L_m}{L_r^2}\Phi_{\beta r} + \frac{1}{\sigma L_s}V_{\beta s} \\ \frac{d\Phi_{\alpha r}}{dt} = \frac{R_r L_m}{L_r}i_{\alpha s} - \frac{R_r}{L_r}\Phi_{\alpha r} - \omega\Phi_{\beta r} \\ \frac{d\Phi_{\beta r}}{dt} = \frac{R_r L_m}{L_r}i_{\beta s} - \frac{R_r}{L_r}\Phi_{\beta r} + \omega\Phi_{\alpha r} \end{cases} \quad (1)$$

where the components $V_{\alpha s}$ and $V_{\beta s}$ define the stator voltage vector, while $i_{\alpha s}$ and $i_{\beta s}$ represent the corresponding elements of the stator current vector. Furthermore, the components $\Phi_{\alpha r}$ and $\Phi_{\beta r}$ characterize the rotor flux vector.

The nonlinear state-space representation of the induction motor is given by [12]–[14],

$$\begin{cases} \frac{dX}{dt} = f(x,U) \\ Y = h(x,U) \end{cases} \quad (2)$$

where

$$X^T = \begin{pmatrix} i_{\alpha s} & i_{\beta s} & \Phi_{\alpha r} & \Phi_{\beta r} \end{pmatrix}, Y = \begin{pmatrix} i_{\alpha s} \\ i_{\beta s} \end{pmatrix}, U = \begin{pmatrix} V_{\alpha s} \\ V_{\beta s} \end{pmatrix}$$

By applying linearization techniques to the nonlinear state model above, the system can be approximated as (3),

$$\begin{cases} \frac{dX}{dt} = AX + BU \\ Y = CX \end{cases} \quad (3)$$

where

$$A = \frac{\partial f}{\partial x}, \quad B = \frac{\partial f}{\partial u}, \quad C = \frac{\partial h}{\partial x} \tag{4}$$

with the system matrices defined by

$$A = \begin{pmatrix} -a & 0 & \frac{R_r L_m}{L_r b} & \omega \frac{L_m}{b} \\ 0 & -a & -\omega \frac{L_m}{b} & \frac{R_r L_m}{L_r b} \\ \frac{R_r L_m}{L_r} & 0 & -\frac{R_r}{L_r} & -\omega \\ 0 & \frac{R_r L_m}{L_r} & +\omega & -\frac{R_r}{L_r} \end{pmatrix}, B = \begin{pmatrix} \frac{1}{\sigma L_s} & 0 \\ 0 & \frac{1}{\sigma L_s} \\ 0 & 0 \\ 0 & 0 \end{pmatrix}, C = \begin{pmatrix} 1 & 0 & 0 & 0 \\ 0 & 1 & 0 & 0 \end{pmatrix}$$

$$a = \frac{1}{\sigma L_s}(R_s + R_r \frac{L_m^2}{L_r^2}) \ , b = \sigma L_s L_r \ , \ \sigma = 1 - \frac{L_m^2}{L_s L_r}$$

These matrices A, B, and C have been characterized in detail in previous studies [3], [15], [16].The model of the rotor current control loop is described as (5),

$$G_i(s) = \frac{V_{ds}}{i_{ds}} = \frac{V_{qs}}{i_{qs}} = \frac{1}{R_r} \cdot \frac{1}{1+\sigma T_s s} \tag{5}$$

where

$$T_s = \frac{L_s}{R_s} \ , \ \sigma = 1 - \frac{L_m^2}{L_s L_r} \text{ and } \ T_m = \frac{J}{f_r}$$

Similarly, the rotational speed control loop can be modeled by (6).

$$G_v(s) = \frac{\omega_r}{C_{em}} = \frac{1}{f_r} \cdot \frac{1}{1+T_m s} \tag{6}$$

2.2. Generalized predictive control (GPC)

The core principle of GPC, like other predictive control strategies, is based on forecasting the future behavior of the process using a process model [17], [18]. The transfer functions describing the dynamics of the induction motor's stator currents and rotational speed are derived from its electrical and mechanical characteristics, as shown in (5) and (6) [19]–[21].

2.2.1. GPC based on quadratic cost minimization

Typically, the GPC cost function comprises quadratic terms penalizing both the control input and the control error [22], [23].

$$J(N_1, N_2) = \sum_{j=N_1}^{N_2} [\hat{y}(t+j) - w(t+j)]^2 + \lambda \sum_{j=1}^{N_u} [u(t+j-1)]^2 \tag{7}$$

We suppose (8).

$$\Delta u(t+j) = 0 \quad \text{for } j \geq N_u \tag{8}$$

N_u denotes the control's horizon; λ refers to the control's weight; w represents an upcoming point or a reference sequence; and $\Delta u(t)$ denotes the control's progressive implementation. Based on the information gathered thus far, $\hat{y}(t+j)$ represents the optimal estimate of a system's output level $\hat{y}(t)$; N_1 and N_2 stand for the lower and higher cost limits, respectively.

2.2.2. GPC for rotor speed and stator current control

The GPC controller for the rotor current loop uses the controlled auto-regressive integrated moving average (CARIMA) model [24]–[26]:

$$A(q^{-1})y(t) = B(q^{-1})u(t-1) + \frac{C(q^{-1})\xi(t)}{\Delta(q^{-1})} \tag{9}$$

where A(q^{-1}) and B(q^{-1}) represent polynomials formulated using the backward shift operator q^{-1} [27]–[29]. Here, $\xi(t)$ denotes zero-mean white noise, u(t) is the control input, and y(t) represents the rotor current in the dq reference frame. The polynomial C(q−1) acts as a filter to mitigate disturbances and measurement noise [30], [31].

The matrix G has a lower-triangular banded structure. This lets us solve the quadratic cost minimization (7) as a linear algebra problem. The optimal solution without constraints is found by using the first-order condition. This means setting the partial derivative of J on Δu to zero [32]–[34]:

$$G = \begin{pmatrix} g_0 & . & . & . & 0 \\ g_1 & g_0 & & . & . \\ g_2 & g_1 & g_0 & . & . \\ . & . & . & . & . \\ g_{N_2-1} & g_{N_2-1} & . & . & g_0 \end{pmatrix} \quad (10)$$

$$u_{\text{opt}} = (G^T G + \lambda I)^{-1} G^T (f - w) \quad (11)$$

Thus, only G and f are needed to determine the optimal control increment vector to apply, which represents the first element of the vector that will be confirmed to apply to the input of the controlled process [35].

$$u(t) = u(t-1) + g^{-T}(f - w) \quad (12)$$

where g^{-T} is the first line of $(G^T G + \lambda I)^{-1} G^T$.

The GPC algorithm is described as in Algorithm 1.

Algorithm 1. GPC algorithm
Beginning
-Obtain the a and b coefficients of the carima type process model
-Calculating polynomial $A.\Delta$
-Resolution of the diophantine equation.
1. define the horizons of predictions and controle as well as the weighting factor.
2. calculation of the polynomial matrices ej and fj
3. calculation of the matrix gj, formation of the matrix g.
4. calculation of the inverse matrix $[G^T G + \lambda . I]^{-1}$
   calculating $[G^T G + \lambda . I]^{-1} G^T$
End

The CGPC approach extends the conventional GPC framework by employing a similar quadratic cost function, while adapting the predictive model to suit the cascaded control architecture. This structural modification ensures that both control layers—the inner and outer loops—operate with distinct prediction models tailored to their respective dynamics.

2.3. Cascaded generalized predictive control

2.3.1. Solving the CGPC

The CGPC approach extends the conventional GPC framework by employing a similar quadratic cost function, while adapting the predictive model to suit the cascaded control architecture. This structural modification ensures that both control layers—the inner and outer loops—operate with distinct prediction models tailored to their respective dynamics. Figure 1 illustrates the general control structure of the proposed CGPC system, designed using PSO.

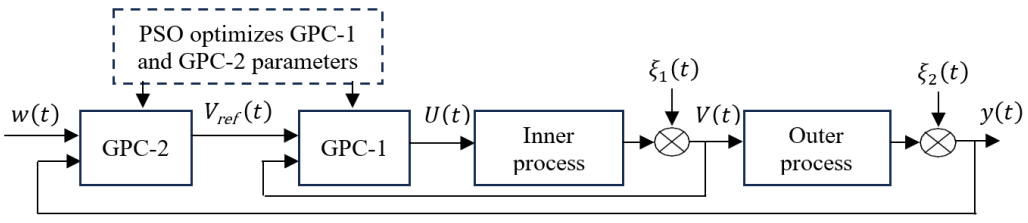

Figure 1. Diagram of the PSO-based cascaded GPC control loop

The CGPC strategy calculates control actions by utilizing both the system's actual output and an intermediate state variable, effectively capturing the interdependence between the loops. This dual-layer predictive mechanism enhances the controller's ability to anticipate future system behavior more accurately by incorporating control inputs, measured outputs, and intermediate references into the prediction process [36], [37]. Within this cascaded configuration, the outer loop GPC governs the external system dynamics (e.g., speed regulation) and the inner loop GPC is responsible for managing the internal system dynamics, such as current control, using its own cost function and predictive setpoints. Figure 2 illustrates the structure of the cascaded PI controllers optimized using the PSO algorithm.

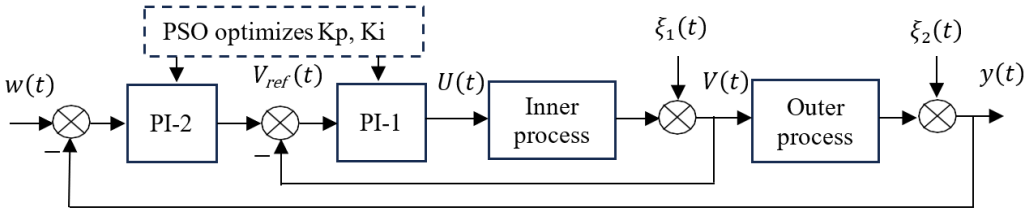

Figure 2. Diagram of the PI controllers' cascaded control loop based on PSO

2.3.2. Cost functions

In a cascaded control structure, two interdependent predictive controllers are used—each responsible for one level of the control hierarchy. Consequently, the CGPC approach involves the formulation and minimization of two distinct quadratic cost functions: one for the outer loop and another for the inner loop. Each cost function adheres to the classical GPC formulation and is designed to penalize deviations from the desired system response while accounting for the control effort.

$$\begin{cases} J_{\text{GPC1}}(N_{11}, N_{21}, N_{u1}) = \sum_{j=N_{11}}^{N_{21}} [w_1(t+j) - \widehat{y_1}(t+j)]^2 + \lambda_1 \sum_{j=1}^{N_{u1}} [\Delta w_2(t+j-1)]^2 \\ J_{\text{GPC2}}(N_{12}, N_{22}, N_{u2}) = \sum_{j=N_{12}}^{N_{22}} \left[w_{2\,opt}(t+j) - \widehat{y_2}(t+j)\right]^2 + \lambda_2 \sum_{j=1}^{N_{u2}} [\Delta u(t+j-1)]^2 \end{cases} \quad (13)$$

where

$\widehat{y_1} = [\widehat{y_1}(t+N_{11})\widehat{y_1}(t+N_{11}+1).....\widehat{y_1}(t+N_{21})]^T$
$\widehat{y_2} = [\widehat{y_2}(t+N_{12})\widehat{y_2}(t+N_{12}+1).....\widehat{y_2}(t+N_{22})]^T$
$\Delta u = [\Delta u(t)\ \Delta u(t+1).....\Delta u(t+N_{u2}-1)]^T$
$w_1 = [w_1(t+N_{11})\ w_1(t+N_{11}+1).....w_1(t+N_{21})]^T$
$w_2 = [w_2(t+N_{12})\ w_2(t+N_{12}+1).....w_2(t+N_{22})]^T$
$\hat{y}_1$and $\hat{y}_2$ represent the future outputs of the external and internal systems, respectively, and
Δw_2: The calculated increments of the future internal setpoint.

2.4. CGPC for linear or nonlinear systems with constraints

The design of the constrained CGPC builds upon the conventional GPC framework, extending it to accommodate both the outer and inner loops of the cascaded structure. In this dual-loop approach, constraints are directly incorporated into each stage of the optimization process, ensuring compliance with physical or operational limitations.

To represent the system dynamics in a more compact and computationally efficient manner, the prediction equations for both loops are derived and expressed in matrix notation as in (14) and (15).

$$\widehat{y_1} = G_1\, \widehat{w_2} + \rho_1 \quad (14)$$

$$\widehat{y_2} = G_2\, \tilde{u} + \rho_2 \quad (15)$$

with:

$\widehat{w_2} = [\Delta w_2(t)\ \Delta w_2(t+1).....\Delta w_2(t+N_{u1}-1)]^T$
$\rho_1 = [\ \rho_{1N_{11}}\ \ \rho_{1N_{11}+1}\ \cdots\cdots\ \rho_{1N_{21}}\ ]^T$
$\rho_2 = [\ \rho_{2N_{12}}\ \ \rho_{2N_{12}+1}\ \cdots\cdots\ \rho_{2N_{22}}\ ]^T$

where $G_1$and G_2 represent the index matrices corresponding to the two subsystems. The first is the criterion defined in (13) can subsequently be expressed in matrix form.

$$\begin{cases} J_1 = [G_1\tilde{w}_2 + \rho_1 - w_1]^T[G_1\tilde{w}_2 + \rho_1 - w_1] + \lambda_1\tilde{w}_2^T\tilde{w}_2 \\ J_2 = [G_2\tilde{u} + \rho_2 - w_2]^T[G_2\tilde{u} + \rho_2 - w_2] + \lambda_2\tilde{u}^T\tilde{u} \end{cases} \quad (16)$$

The second one is the optimal solution is determined by first minimizing J_1, followed by minimizing J_2 based on the outcome of the first minimization; this sequential optimization yields the control input applied to the system.

$$\frac{\partial J_{GPC1}}{\partial \tilde{w}_2} = 0$$

$$J_1 \Rightarrow \tilde{w}_{2\,opt} = [G_1^T\, G_1 + \lambda_1 I_{N_{u1}}]^{-1}\, G_1^T\, [w_1 - \rho_1]$$

$$\frac{\partial J_{GPC2}}{\partial \tilde{u}} = 0$$

$$J_2 \Rightarrow \tilde{u}_{\,opt} = [G_2^T\, G_2 + \lambda_2 I_{N_{u2}}]^{-1}\, G_2^T\, [\tilde{w}_{2\,opt} - \rho_2]$$

At each step, only the first control action from the optimized sequence is implemented on the system [38].

$$u_{opt}(t) = u_{opt}(t\ -\ 1)\ + 1^{\text{st}}\, line\left\{\left[G_2^T G_2 + \lambda_2 I_{N_{u_2}}\right]^{-1} G_2^T\left(w_{2\,opt} - \rho_2\right)\right\}$$

2.5. Overview of particle swarm optimization with penalty factor-based constraint handling

PSO is a population-based optimization technique inspired by the collective dynamics seen in social organisms, such as bird flocks and fish schools. Due to its intuitive structure and strong performance, PSO has become a popular method for solving a wide range of optimization problems, both constrained and unconstrained, across various engineering disciplines.

In its standard form, an unconstrained optimization problem can be formulated as (17).

$$min\, J(X_i) = f(X_i), \quad X_i = [x_i^1, x_i^2, \ldots\ldots, x_i^n] \quad (17)$$

Subject to $g_j(X_i) \leq 0$ for j = 1, 2,…, K.

In this formulation, $f(X_i)$ represents the objective (cost) function, and $x \in R^n$ denotes the decision variable vector associated with the i-th particle. The inequality constraints $g_j(X_i)$ define the feasible region of the search space.

The constraint formulation in (17) is flexible and not restrictive. For instance, an inequality constraint of the form $g_j(X_i) \geq 0$ can be equivalently rewritten as $-g_j(X_i) \leq 0$. Similarly, an equality constraint $g_j(X_i) = 0$ can be represented as two simultaneous inequalities: $g_j(X_i) \leq 0$ and $-g_j(X_i) \leq 0$.

In the standard formulation of the PSO algorithm, each particle represents a potential solution and updates its velocity and position iteratively. This update process is influenced by both its own personal best position and the best position found by the entire swarm (global best) [39]. The evolution of the particle's velocity and position is governed by (18) and (19).

$$V_i(t+1) = w_1 V_i(t) + c_1 R_1\left(P_i - X_i(t)\right) + c_2 R_2\left(P_g - X_i(t)\right) \quad (18)$$

$$X_i(t+1) = X_i(t) + V_i(t+1) \quad (19)$$

Here, $V_i = [v_i^1, v_i^2, \ldots\ldots, v_i^N]$ represents the velocity of particle *i*, and $X_i = [x_i^1, x_i^2, \ldots\ldots, x_i^n]$ denotes its current position. P_i denotes the personal best position previously encountered by the particle, reflecting its most successful prior experience. Pg represents the globally best position discovered by the swarm, corresponding to the most optimal solution found up to the current iteration. The inertia weight w governs the influence of a particle's previous velocity on its current trajectory and can be adaptively tuned to balance exploration and exploitation [40].

The coefficients R_1 and R_2 are independently drawn from a uniform distribution over the interval [0, 1]. This randomness can sometimes cause excessive variation in the particle's trajectory. The learning rates are represented by the positive constant parameters C_1 and C_2.

To prevent particles from drifting too far outside the search space, the velocity components V_i are typically constrained within predefined bounds $[-V_{min}, V_{max}]$ [15]. To account for constraints, a penalty method is employed by modifying the cost function in (20).

$$F(X) = f(X) + \sum_{j=1}^{k} P_j \left| g_j(X) \right| \quad (20)$$

The penalty coefficient P_j is defined as (21).

$$P_j = \begin{cases} h_j & if \quad g_j(X) > 0 \\ 0 & otherwise \end{cases} \quad (21)$$

2.6. CGPC with limitations for linear or nonlinear processes based on PSO

Using the cost function (7) alone to capture the plant's operational requirements is challenging, particularly when generating the control signal as outlined in (11). To more accurately represent these requirements, additional constraints, such as those related to white noise, must be incorporated into the control design. In some cases, additional constraints related to the system's output can also be introduced to better meet the system's specifications. Research on constrained PSO [41], [42] indicates that incorporating multiple constraints results in only a modest increase in computational complexity. This makes constrained PSO a more efficient alternative compared to traditional methods like LMI approaches [43]. Consequently, as long as the dynamic models are sufficiently accurate, the proposed method is adaptable to any modeling approach, whether linear or nonlinear, and can be applied in both offline and online scenarios.

$$\Delta_u (K + j - 1), j = 1,2, \ldots \ldots, N_u \quad (22)$$

The cost function h_i may also be simplified by omitting the term associated with the control signal, as shown in (23).

$$\lambda \sum_{j=1}^{N_u} [\Delta_u (t + j - 1)]^2 \quad (23)$$

The intelligent GPC with constraints defines the cost function (24). The diagram of GPC with constrained based on PSO is shown by Figure 3.

$$\sum_{j=1}^{N} [\hat{y}(t + j) - w(t + j)]^2 \quad (24)$$

Several constraints are proposed for the induction motor drive system, from the point of view of the '$\lambda \sum_{j=1}^{N_u} [\Delta_u (t + j - 1)]^2$' approach. They are as follows.

- The system specifics define the range of control signals: $R_1 \leq R_2$, where R_1 and R_2 are determined by the system characteristics.
- The control signals' first-order differential value is $|\Delta_u| \leq D_1$, where D_1 is a positive constant.
- The control signals' second-order differential value is $|\Delta\Delta_u| \leq D_2$, where D_2 is a positive constant.

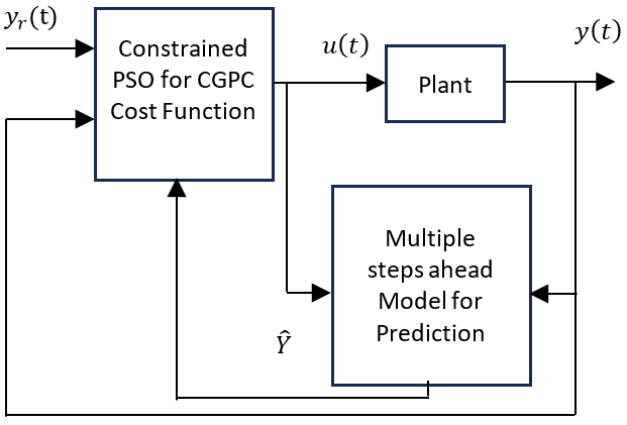

Figure 3. CGPC Structure based on PSO with constraints

These constraints have clear physical interpretations and can be easily implemented in practice. Moreover, additional constraints on the system's output can be integrated without significantly increasing computational complexity, which offers a distinct advantage over methods like Linear Matrix Inequality (LMI) techniques [44], [45].

It is crucial to note that the system identification method is not a critical factor for this approach; any accurate model—whether linear or nonlinear, and whether obtained offline or online—can be used within the constrained CGPC-PSO framework. The CGPC controller, employed to regulate both the speed and current of the induction motor drive, incorporates a PSO-based constraint, as illustrated in Figure 4.

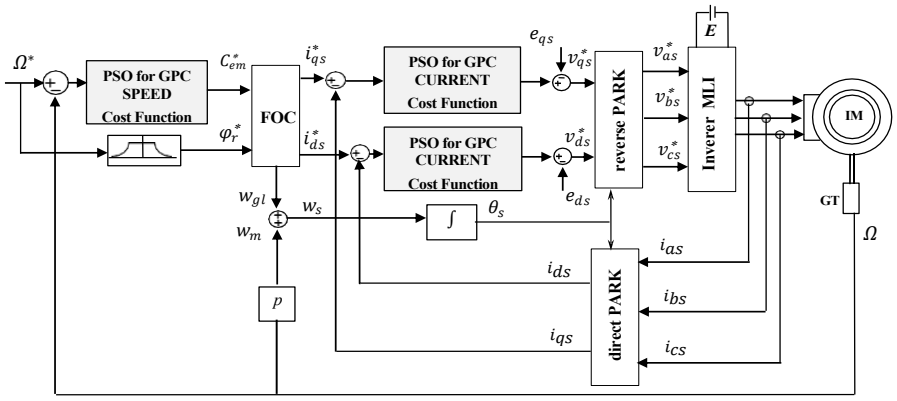

Figure 4. CGPC with PSO-based constraints applied in induction motor drive

3. SIMULATIONS RESULTS

Simulation tests were conducted on an induction motor powered by a standard three-phase 220/380 V power supply to evaluate the performance of the proposed GPC approach, considering both its cascaded structure and the application of constraints.

Figures 5 and 6 illustrate two different test scenarios designed to assess the dynamic response and robustness of the GPC controllers. For clarity, GPC0 represents the system without the cascaded structure, and GPC1 represents the system with the cascaded structure. Figure 5 shows a no-load startup scenario. The motor is commanded to reach a target speed of 400 rpm, followed by the application of a nominal load torque of 5 Nm at t = 0.3 s, which is maintained for 0.3 seconds. The results demonstrate quick convergence to the desired speed and effective disturbance rejection during the load torque application for both GPC0 and GPC1. Figure 6 depicts a speed reversal test, in which the reference speed alternates between +600 rpm and -600 rpm. The simulation scenario includes a no-load start, the application of a resistive load between 0.35 s and 0.75 s, and a reversal of the direction of rotation between 1 s and 2 s. The motor tracks the commanded speed with minimal overshoot and a short settling time for both GPC0 and GPC1. This scenario further highlights the controller's excellent disturbance rejection capabilities and effective decoupling between flux and torque, validating the performance of the cascaded GPC structure in GPC1.

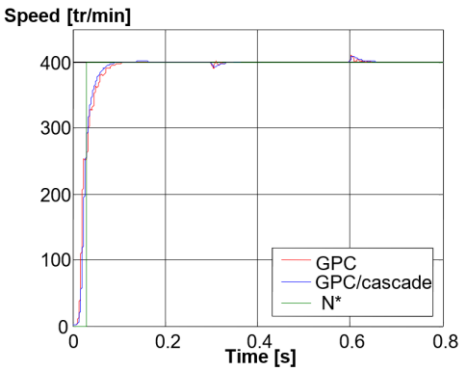

Figure 5. Comparison between GPC controller and CGPC with constraints

Overall, the simulation results confirm that the GPC controllers, both with and without cascading (GPC0 and GPC1), successfully achieve precise speed control under dynamic conditions, demonstrating their robustness and adaptability in managing various operational constraints. The parameters of the induction motor used in the simulation are listed in Table 1.

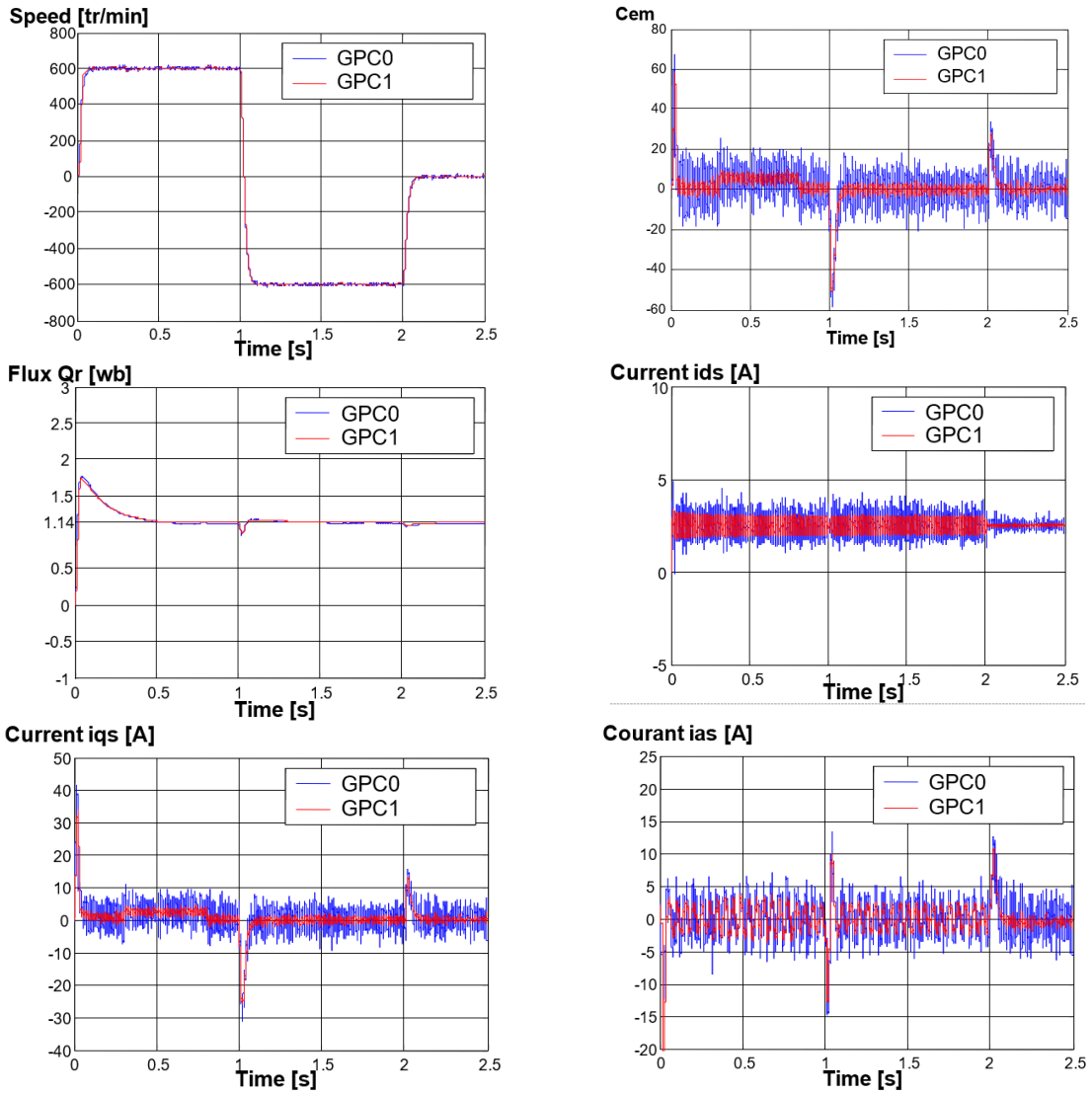

Figure 6. Simulation results of the asynchronous machine drive under cascaded GPC control

Table 1. Induction motor parameters

Parameter	Value
Rated power	1.1Kw
Rated voltage	220/380 V-50 Hz
Rated speed	1000 tr/mn
Rated torque	7 Nm
Stator resistance	8.1 Ω
Rotor resistance	3.2 Ω
Stator inductance	0.48 H
Rotor inductance	0.48 H
Mutual Inductance	0.46 H
Moment of inertia	0.006 kg.m^2
Coefficient of viscous friction	0.005 Nm/(rad/s)
Number of poles	3

4. COMPARISON WITH EXISTING APPROACHES AND CONTRIBUTIONS

4.1. Comparison with existing approaches

The proposed CGPC PSO method advances beyond previous control strategies in several keyways: unlike PSO GPC approaches—such as Otmane [46], which optimized GPC parameters without explicit input/output constraint handling, and He *et al.* [6], which struggled with real-time computation and resilience in perturbed MIMO environments—CGPC PSO robustly manages constraints and adapts online; compared

with LMI based MPC methods (e.g. Kim and Kim [7]) that, although ensuring constraint satisfaction, impose prohibitive computational complexity for real-time deployment, and hybrid LMI convex MPC designs [8] that falter in highly nonlinear or cascade-structured systems, CGPC PSO maintains both rigor and efficiency; and versus neural predictive control strategies like Stiti *et al.* [9], whose neural network models require retraining for each new system, and Wang *et al*. [10], whose neural-MPC variants lack effective real-time adaptation under dynamic conditions, our approach offers generalizable, flexible prediction and adaptation with improved robustness—demonstrating clear computational, adaptability, and performance advantages.

4.2. Contribution

The contributions of CGPC-PSO stand out when compared to existing methods. On the one hand, it combines the simplicity and efficiency of PSO for optimizing predictive controllers while explicitly managing constraints. On the other hand, it is less complex than LMI-based solutions and more robust than neural approaches, which may suffer from limited generalization. Furthermore, the CGPC-PSO method offers significant flexibility in terms of structure and adaptability, making it particularly suitable for real-time industrial systems.

5. DISCUSSION

The present work addresses the scientific question of how to enhance robustness, constraint management, and transient performance of GPC applied to induction motor drives. The study specifically explores the potential of PSO to automatically tune key predictive parameters—such as the prediction horizons and weighting coefficients—so as to achieve optimal control performance without increasing computational complexity.

The results clearly demonstrate that the proposed CGPC optimized by PSO (CGPC–PSO) provides significant performance improvements compared with conventional PI and standard GPC controllers. Through the optimal selection of predictive parameters by PSO, the CGPC–PSO reduces overshoot by nearly 80%, halves the settling time, and minimizes the steady-state error. Furthermore, the proposed approach maintains stability and tracking accuracy under variations in load torque and machine parameters, validating its robustness and adaptability.

The conclusions are supported by both analytical derivations and simulation-based evidence. The theoretical modeling of the induction motor in the (α, β) reference frame forms the foundation for the CGPC formulation. The PSO algorithm is then employed to optimize the predictive control law with respect to a cost function that balances tracking precision, control smoothness, and constraint satisfaction. Comparative MATLAB/Simulink simulations with PI, GPC, and CGPC–PSO controllers under identical operating conditions—such as speed reversal and load disturbances—demonstrate the superior dynamic and steady-state performance of the proposed method.

The significance of these results extends beyond the context of induction motor drives. The integration of metaheuristic optimization into predictive control design opens new perspectives for intelligent and adaptive control of constrained systems. In particular, the CGPC–PSO provides a computationally efficient alternative to LMI-based MPC, while avoiding the retraining complexity of neural-based MPC methods. This makes the approach suitable for real-time applications in renewable energy systems, electric vehicle propulsion, and industrial automation, where robustness and efficiency are essential.

This study, conducted in simulation, provides a solid foundation for future experimental validation. The CGPC–PSO controller can be implemented on DSP or FPGA platforms. Future work will focus on hardware-in-the-loop testing, comparison with other metaheuristic optimizers (JAYA, GWO), and consideration of nonlinear effects, aiming to confirm the controller's reliability and extend its applicability to real industrial and robotic scenarios.

In summary, the integration of PSO-based optimization into predictive control provides a computationally efficient and robust framework for constrained systems. CGPC–PSO offers a practical alternative to LMI-based MPC while avoiding the retraining complexity of neural MPC, making it suitable for real-time applications across industrial, robotic, and automated platforms.

6. CONCLUSION

The CGPC technique, enhanced by the PSO algorithm, has been introduced as an effective solution for managing heavily loaded induction motor drives (IMD). This approach simplifies control design by leveraging the advantages of PSO, eliminating the need for complex mathematical formulations, and providing a practical, yet robust, solution for real-world control challenges.

Performance evaluations through numerical simulations demonstrate that the CGPC-PSO controller excels in precise tracking, maintains robustness under varying operating conditions, and effectively handles operational constraints. Moreover, its low computational overhead and ease of implementation make it a promising solution for practical applications.

Looking ahead, integrating this approach with other artificial intelligence techniques—such as fuzzy logic, neural networks, or genetic algorithms—could further enhance the system's adaptability and performance. Such hybrid strategies could optimize parameter tuning and further improve robustness. Additionally, transitioning from simulation-based tests to real-world experimental setups will be a crucial next step to validate the controller's effectiveness in real-time environments.

Other potential future directions include i) extending the control framework to multi-motor systems or complex industrial drives, which require coordination and synchronization; ii) exploring fault-tolerant control strategies to improve system reliability, especially in the presence of sensor or actuator failures; and iii) incorporating energy efficiency objectives into the control design to reduce power consumption while ensuring high performance.

FUNDING INFORMATION

This work received no external funding.

AUTHOR CONTRIBUTIONS STATEMENT

This journal uses the Contributor Roles Taxonomy (CRediT) to recognize individual author contributions, reduce authorship disputes, and facilitate collaboration.

Name of Author	C	M	So	Va	Fo	I	R	D	O	E	Vi	Su	P	Fu
Rachid Amrouche	✓	✓	✓	✓	✓	✓		✓	✓	✓	✓		✓	
Noureddine Boumalha			✓	✓		✓		✓	✓		✓	✓	✓	
Farid Ykhlef	✓		✓	✓		✓			✓	✓		✓	✓	
Djilali Kouchih		✓		✓	✓		✓		✓		✓			
Author x name					✓		✓			✓		✓		

C : **C**onceptualization
M : **M**ethodology
So : **So**ftware
Va : **Va**lidation
Fo : **Fo**rmal analysis
I : **I**nvestigation
R : **R**esources
D : **D**ata Curation
O : Writing - **O**riginal Draft
E : Writing - Review & **E**diting
Vi : **Vi**sualization
Su : **Su**pervision
P : **P**roject administration
Fu : **Fu**nding acquisition

CONFLICT OF INTEREST STATEMENT

The authors declare no conflict of interest.

DATA AVAILABILITY

The author(s) has(have) no permission to share the data.

REFERENCES

[1] D. W. Clarke, C. Mohtadi, and P. S. Tuffs, "Generalized predictive control—Part I. The basic algorithm," *Automatica*, vol. 23, no. 2, pp. 137–148, Mar. 1987, doi: 10.1016/0005-1098(87)90087-2.

[2] D. W. Clarke, C. Mohtadi, and P. S. Tuffs, "Generalized predictive control—Part II Extensions and interpretations," *Automatica*, vol. 23, no. 2, pp. 149–160, Mar. 1987, doi: 10.1016/0005-1098(87)90088-4.

[3] K. K. Otmane, "Anti-saturation GPC speed control of induction motor drives," *The Journal of Engineering*, vol. 2022, no. 5, pp. 459–465, May 2022, doi: 10.1049/tje2.12129.

[4] Z. Zhang, A. H. D. Christensen, S. Hørsholt, and J. B. Jørgensen, "Numerical discrete-time implementation of continuous-time linear-quadratic model predictive control," Mar. 2025, [Online]. Available: http://arxiv.org/abs/2407.18825

[5] J. B. Oliveira, J. Boaventura-Cunha, P. B. Moura Oliveira, and H. Freire, "A swarm intelligence-based tuning method for the sliding mode generalized predictive control," *ISA Transactions*, vol. 53, no. 5, pp. 1501–1515, Sep. 2014, doi: 10.1016/j.isatra.2014.06.007.

[6] N. He, D. Shi, M. Forbes, J. Backström, and T. Chen, "Robust tuning for machine-directional predictive control of MIMO paper-making processes," *Control Engineering Practice*, vol. 55, pp. 1–12, Oct. 2016, doi: 10.1016/j.conengprac.2016.06.008.

[7] D.-J. Kim and B. Kim, "Linear matrix inequality-based robust model predictive speed control for a permanent magnetic synchronous motor with a disturbance observer," *Energies*, vol. 17, no. 4, p. 869, Feb. 2024, doi: 10.3390/en17040869.

[8] I. Nodozi and M. Rahmani, "LMI-based model predictive control for switched nonlinear systems," *Journal of Process Control*, vol. 59, pp. 49–58, Nov. 2017, doi: 10.1016/j.jprocont.2017.09.001.

[9] C. Stiti *et al.*, "Lyapunov-based neural network model predictive control using metaheuristic optimization approach," *Scientific Reports*, vol. 14, no. 1, p. 18760, Aug. 2024, doi: 10.1038/s41598-024-69365-9.

[10] D. Wang *et al.*, "Model predictive control using artificial neural network for power converters," *IEEE Transactions on Industrial Electronics*, vol. 69, no. 4, pp. 3689–3699, Apr. 2022, doi: 10.1109/TIE.2021.3076721.

[11] A. Belbali, S. Makhloufi, A. Kadri, L. Abdallah, and Z. Seddik, "Mathematical modeling of a three-phase induction motor," in *Induction Motors - Recent Advances, New Perspectives and Applications*, IntechOpen, 2023. doi: 10.5772/intechopen.1001587.

[12] K. Ouari *et al.*, "Improved nonlinear generalized model predictive control for robustness and power enhancement of a DFIG-based wind energy converter," *Frontiers in Energy Research*, vol. 10, Sep. 2022, doi: 10.3389/fenrg.2022.996206.

[13] Z. Németh and M. Kuczmann, "State space modeling theory of induction machines," *Pollack Periodica*, vol. 15, no. 1, pp. 124–135, Apr. 2020, doi: 10.1556/606.2020.15.1.12.

[14] S. I. Khather, M. A. Ibrahim, and A. I. Abdullah, "Review and performance analysis of nonlinear model predictive control—current prospects, challenges and future directions," *Journal Européen des Systèmes Automatisés*, vol. 56, no. 4, pp. 593–603, Aug. 2023, doi: 10.18280/jesa.560409.

[15] K. M. Anstreicher, "Semidefinite programming versus the reformulation-linearization technique for nonconvex quadratically constrained quadratic programming," *Journal of Global Optimization*, vol. 43, no. 2–3, pp. 471–484, Mar. 2009, doi: 10.1007/s10898-008-9372-0.

[16] I. Miloud, S. Cauet, E. Etien, J. P. Salameh, and A. Ungerer, "Real-time speed estimation for an induction motor: an automated tuning of an extended Kalman filter using voltage–current sensors," *Sensors*, vol. 24, no. 6, p. 1744, Mar. 2024, doi: 10.3390/s24061744.

[17] Wei Gao, Miao-Lei Zhou, Yuan-Chun Li, and Tao Zhang, "An adaptive generalized predictive control of time-varying delay system," in *Proceedings of 2004 International Conference on Machine Learning and Cybernetics (IEEE Cat. No.04EX826)*, vol. 2, pp. 878–881. doi: 10.1109/ICMLC.2004.1382309.

[18] R. Cordero, M. Caramalac, and W. Ali, "Generalized predictive control with added zeros and poles in its augmented model for power electronics applications," *Energies*, vol. 17, no. 23, p. 6037, Dec. 2024, doi: 10.3390/en17236037.

[19] S. Chirantan and B. B. Pati, "Torque and d-q axis current dynamics of an inverter fed induction motor drive that leverages computational intelligent techniques," *AIMS Electronics and Electrical Engineering*, vol. 8, no. 1, pp. 28–52, 2024, doi: 10.3934/electreng.2024002.

[20] P. C. Krause, O. Wasynczuk, S. D. Sudhoff, and S. Pekarek, *Analysis of electric machinery and drive systems*, vol. 2. Wiley Online Library, 2002.

[21] D. Yang, Z. Kan, Y. Wang, W. Ren, Y. Yang, and K. Xia, "Small-signal input impedance modeling of PWM induction motor drives and interactive stability assessment with DC link," *Machines*, vol. 13, no. 7, p. 580, Jul. 2025, doi: 10.3390/machines13070580.

[22] A. Elmouatamid, R. Ouladsine, M. Bakhouya, N. El kamoun, and K. Zine-Dine, "A predictive control strategy for energy management in micro-grid systems," *Electronics*, vol. 10, no. 14, p. 1666, Jul. 2021, doi: 10.3390/electronics10141666.

[23] M. J. Memeghani, S. M. Ghamari, T. Y. Jouybari, H. Mollaee, and P. Wheeler, "Generalised predictive controller (GPC) design on single-phase full-bridge inverter with a novel identification method," *IET Control Theory & Applications*, vol. 17, no. 3, pp. 284–294, Feb. 2023, doi: 10.1049/cth2.12295.

[24] A. Ramdani and S. Grouni, "Dynamic matrix control and generalized predictive control, comparison study with IMC-PID," *International Journal of Hydrogen Energy*, vol. 42, no. 28, pp. 17561–17570, Jul. 2017, doi: 10.1016/j.ijhydene.2017.04.015.

[25] X. Yu, Q. Zhao, C. Gao, L. Zhang, Y. Wu, and H. Nan, "Generalized predictive control of doubly fed variable-speed pumped storage unit," *Energies*, vol. 18, no. 11, p. 2904, Jun. 2025, doi: 10.3390/en18112904.

[26] D. Naunay, P. Ayala, J. Andino, W. Martinez, and D. Arcos-Aviles, "Generalized predictive control for a single-phase, three-level voltage source inverter," *Energies*, vol. 18, no. 10, p. 2541, May 2025, doi: 10.3390/en18102541.

[27] H. Zamani, K. Abbaszadeh, M. Karimi, and J. Gyselinck, "Offset free generalized model predictive control for 3-phase LCL-filter based grid-tied inverters," *International Journal of Electrical Power & Energy Systems*, vol. 153, p. 109351, Nov. 2023, doi: 10.1016/j.ijepes.2023.109351.

[28] P. Rodriguez and D. Dumur, "Generalized predictive control robustification under frequency and time-domain constraints," *IEEE Transactions on Control Systems Technology*, vol. 13, no. 4, pp. 577–587, Jul. 2005, doi: 10.1109/TCST.2005.847330.

[29] A. Bektache, H. Achouri, and K. S. Belkhir, "Robust nonlinear predictive control applied to induction motors," *Engineering, Technology & Applied Science Research*, vol. 13, no. 3, pp. 10951–10956, Jun. 2023, doi: 10.48084/etasr.5732.

[30] Y. Wang, Y. Wang, X. Chen, Y. Wang, and A. Ma, "Research on improved GPC of pantograph considering actuator time delay and external disturbance," *Sensors*, vol. 24, no. 22, p. 7350, Nov. 2024, doi: 10.3390/s24227350.

[31] L. Yin, G. Zhang, and H. Gao, "Estimation of ARMAX processes with noise corrupted output signal observations," *Journal of the Franklin Institute*, vol. 360, no. 12, pp. 8363–8381, Aug. 2023, doi: 10.1016/j.jfranklin.2023.06.032.

[32] P. Rodríguez, D. Dumur, and S. Font, "Youla parametrization applied to a GPC controlled SISO system," *IFAC Proceedings Volumes*, vol. 35, no. 1, pp. 291–296, 2002, doi: 10.3182/20020721-6-ES-1901.00617.

[33] J. N. Strohm and B. Lohmann, "Optimal feedforward preview control by FIR filters," *IFAC-PapersOnLine*, vol. 50, no. 1, pp. 5115–5120, Jul. 2017, doi: 10.1016/j.ifacol.2017.08.779.

[34] T. Wang *et al.*, "Multivariable generalised predictive control with measurement noise rejection and speed ripple mitigation for PMSM drives," *IET Power Electronics*, vol. 13, no. 12, pp. 2607–2617, Sep. 2020, doi: 10.1049/iet-pel.2020.0246.

[35] E. F. Camacho and C. B. Alba, *Model predictive control*, 2nd ed. Springer London, 2004. [Online]. Available: https://books.google.co.id/books?id=tXZDAAAAQBAJ

[36] I. Benyó, J. Kovács, M. Paloranta, and U. Kortela, "Cascade generalized predictive controller: two in one," *International Journal of Control*, vol. 79, no. 8, pp. 866–876, Aug. 2006, doi: 10.1080/00207170600678249.

[37] T. Geng and J. Zhao, "Adaptive cascade generalized predictive control," *International Journal of Intelligence Science*, vol. 04, no. 03, pp. 70–79, 2014, doi: 10.4236/ijis.2014.43009.

[38] M. Sedraoui, S. Abdelmalek, and S. Gherbi, "Multivariable generalized predictive control using an improved particle swarm optimization algorithm," *Informatica*, vol. 35, no. 3, 2011.

[39] S. Chen, N.-Y. Li, V. M. Preciado, and N. Matni, "Robust model predictive control of time-delay systems through system level synthesis," Sep. 2022, [Online]. Available: http://arxiv.org/abs/2209.11841

[40] J. Zhang, Y. Zhai, Z. Han, and J. Lu, "Improved particle swarm optimization based on entropy and its application in implicit generalized predictive control," *Entropy*, vol. 24, no. 1, p. 48, Dec. 2021, doi: 10.3390/e24010048.

[41] J. Smoczek and J. Szpytko, "Particle swarm optimization-based multivariable generalized predictive control for an overhead crane," *IEEE/ASME Transactions on Mechatronics*, vol. 22, no. 1, pp. 258–268, Feb. 2017, doi: 10.1109/TMECH.2016.2598606.

[42] A. Zahaf, A. Abboudi, A. Bounemeur, S. Bououden, and M. Chemachema, "A constrained PSO based model predictive control for mobile robot system with sensor faults," 2024, pp. 333–342. doi: 10.1007/978-981-97-0045-5_31.
[43] Q. Fu, S. Li, Y. Hu, Y. Zhang, and W. Liu, "Algorithm of constrained generalized predictive control based on PSO-SA," in *2010 Chinese Control and Decision Conference*, May 2010, pp. 3046–3051. doi: 10.1109/CCDC.2010.5498662.
[44] C. A. Kedir and C. M. Abdissa, "PSO based linear parameter varying-model predictive control for trajectory tracking of autonomous vehicles," *Engineering Research Express*, vol. 6, no. 3, p. 035229, Sep. 2024, doi: 10.1088/2631-8695/ad722e.
[45] K. Barra and K. Benmahammed, "Cascaded predictive control CGPC of an induction motor drive under constrained efficiency optimisation," in *IECON 2006 - 32nd Annual Conference on IEEE Industrial Electronics*, Nov. 2006, pp. 1316–1321. doi: 10.1109/IECON.2006.347689.
[46] K. K. Otmane, "Anti windup GPC speed controller for induction machine based on Youla parametrization," *Journal of Electrical Engineering*, vol. 73, no. 1, pp. 50–56, Feb. 2022, doi: 10.2478/jee-2022-0007.

BIOGRAPHIES OF AUTHORS

Rachid Amrouche received the engineer degree in electronics (communication option) in 2002, and the magister degree in Instrumentation and Microelectronics in 2016, both from the University of Medea, Algeria. He is currently pursuing a Ph.D. in automatic control and electrical engineering at the University of Blida 1, Algeria. His research interests include model predictive control, constrained control of electrical drives, induction motor drives, optimization-based control techniques, and the application of particle swarm optimization to advanced control systems. He can be contacted at rachamrouche1976@gmail.com.

Noureddine Boumalha received the engineer degree, the magister degree in Electrical Engineering from the University of Medea, Algeria, in 2005 and 2010, respectively. Since 2006, he has been an engineer of maintenance at Mediterranean Float Glass Company. He is currently pursuing a Ph.D. in the automatic department of the National Polytechnic School (ENP), Algiers. His research interests are in the area of electrical drives, process control, diagnosis, and fault tolerant control of wind energy systems. He can be contacted at boumalhanoureddine@gmail.com.

Farid Ykhlef was initially employed as a researcher in 2003 by the Research Center in Industrial Technologies (CRTI), Algiers, Algeria. In 2004, he joined the University of Blida, where he worked as an assistant professor at the Department of Electronics and a researcher at the Laboratory of Signal and Image Processing (LATSI). He was promoted to associate professor in 2014 and then to full professor in 2021. His current research interests include signal processing and artificial intelligence. He can be contacted at f_ykhlef@yahoo.fr.

Djilali Kouchih is a professor in the Automatic and Electrotechnics Department at the University Blida 1, Algeria. He received the engineer degree, the Ph.D. degree in electrical engineering from the National Polytechnics School of Algiers, Algeria, in 1994 and 2015, respectively. His research interests are in the area of electrical drives, process control, diagnosis, and renewable energies. He can be contacted at djkouchih@yahoo.fr.